Heliyon 8 (2022) e12108

Contents lists available at ScienceDirect

Heliyon

journal homepage: www.cell.com/heliyon

Research article

Pan-cancer analysis of LINC02535 as a potential biomarker and its oncogenic role in lung adenocarcinoma

Shuang Dai [a,1], Tao Liu [b,1], Ying-Ying He [c], Yan Huang [a], Li Wang [a], Feng Luo [a], Yan Li [d,*]

[a] Department of Medical Oncology, Lung Cancer Center, West China Hospital, Sichuan University, Chengdu, Sichuan Province, PR China
[b] Department of Oncology, Clinical Medical College and the First Affiliated Hospital of Chengdu Medical College, Key Clinical Specialty of Sichuan Province. Chengdu, Sichuan Province, PR China
[c] Oncology Department, People`s Hospital of Deyang City, Deyang, Sichuan Province, PR China
[d] Department of Radiation Oncology, Lung Cancer Center, West China Hospital, Sichuan University, Chengdu, Sichuan Province, PR China

ARTICLE INFO

Keywords:
Pan-cancer
Lung adenocarcinoma
LINC02535
Epithelial-mesenchymal transition
CD73

ABSTRACT

Background: LINC02535 has gained much attention for its oncogenicity across several cancers, but the systematic pan-cancer analysis of LINC02535 has not been carried out before.

Methods: Herein, we explored the expression level, prognostic value, and hallmark pathways of LINC02535 across multiple cancers using the Cancer Genome Atlas (TCGA) and Cancer Cell Line Encyclopedia (CCLE) databases. Moreover, the expression and biological features of LINC02535 in lung adenocarcinoma (LUAD) were confirmed by qRT-PCR, *in vitro* and *in vivo* experiments.

Results: LINC02535 is differentially expressed in 10 of 17 human cancers and serves as a favorable or unfavorable biomarker in distinct cancer types. Gene set enrichment analysis (GSEA) indicated that key oncogenic pathways/phenotypes were remarkably activated in most cancers with intratumoral increased LINC02535, whereas these pathways/phenotypes were suppressed in other cancer types (colon adenocarcinoma, kidney renal clear cell carcinoma, rectal adenocarcinoma) with intratumoral decreased LINC02535. Of note, the epithelial-mesenchymal transition (EMT) phenotype was greatly enriched in LUAD patients with elevated LINC02535. Based on the TCGA and CCLE datasets, LINC02535 was positively correlated with the EMT-related gene CD73 (also named as NT5E, an immunosuppressive gene) in almost all cancer types (Spearman $R > 0.5$, $P < 0.001$) including LUAD. Most importantly, qRT-PCR confirmed that LINC02535 was upregulated in lung cancer cells or tissues as opposed to human bronchial epithelial cells or paratumor tissues. Knockdown of LINC02535 inhibited proliferation, migration of LUAD cells and retarded xenografted tumor growth. Moreover, silencing of LINC02535 induced apoptosis and cell cycle arrest at G1 phase.

Conclusions: The findings from our pan-cancer analysis provide a relatively comprehensive understanding of the potential value of LINC02535 across multiple cancers, and the oncogenic role of LINC02535 in LUAD has been confirmed.

1. Introduction

Nowadays cancer has always been the major public health problem worldwide because it is a leading cause of mortality globally [1, 2]. Lung cancer ranks first among all malignancies in both morbidity and mortality, and the morbidity and mortality of lung cancer show an increasing trend [1]. Global cancer statistics from the International Agency for Research on Cancer (IARC) estimated that cancer deaths in 2020 were up to 10 million, and lung cancer remained the first cancer death with mortality rate of about 18% [1]. In the past two decades, the discovery of driver genes has greatly contributed to treatment efficacy of cancer, especially lung cancer, and opened a new era of individualized and precise treatment. However, owing to distant metastases of brain, bone and other organs, advanced cancer patients not only lost opportunity of surgical resection but suffered from drug failure and tumor relapse [3, 4]. Therefore, it is of great clinical significance to investigate the molecular mechanisms of carcinogenesis and to screen new targets for cancer therapy.

* Corresponding author.
E-mail address: liyan1240@wchscu.cn (Y. Li).
[1] These authors have contributed equally to this work and share first authorship.

https://doi.org/10.1016/j.heliyon.2022.e12108
Received 30 July 2022; Received in revised form 6 November 2022; Accepted 28 November 2022

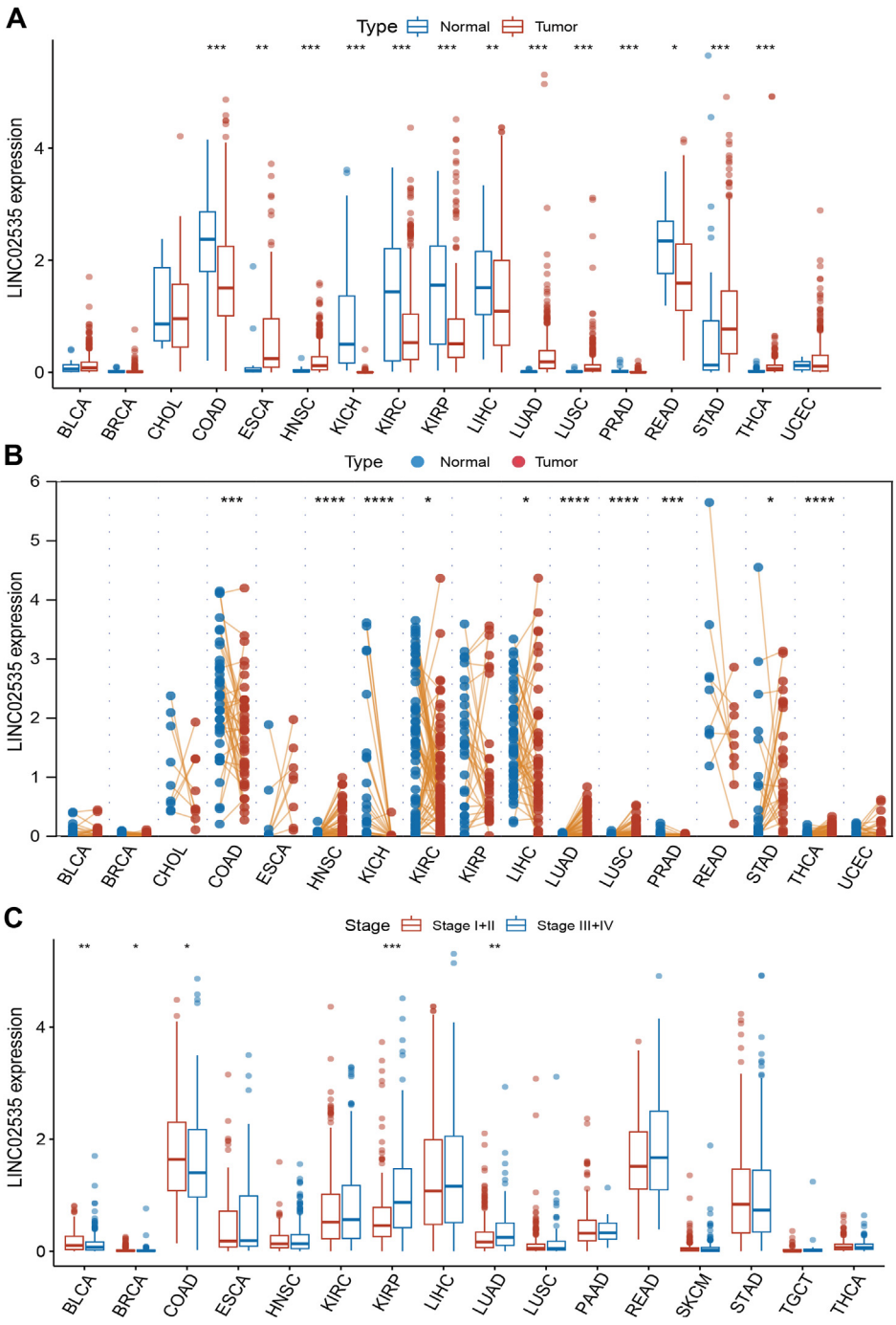

Figure 1. Expression pattern and prognostic analysis of LINC02535 in pan-cancers. (A) LINC02535 expression in cancer and normal tissues from TCGA database; (B) LINC02535 expression across paired cancer and corresponding para-cancer tissues; (C) LINC02535 affects lung cancer progression. *$P < 0.05$, ** $P < 0.01$, *** $P < 0.001$, **** $P < 0.0001$.

Long noncoding RNA (lncRNA) with a length of more than 200nt, accounting for over 70% of human genome, was previously regarded as transcriptional "noise" without function [5, 6, 7]. In recent years, researchers have found that lncRNA can regulate the expression and localization of protein-coding genes across multiple tumors, and plays a pro-tumor role in tumor growth, angiogenesis, invasion and metastasis [8, 9, 10, 11, 12]. Of note, LINC02535, one of intergenic region lncRNA, is located on chromosome 6q14.3, and contains two transcripts with lengths of 2529bp and 2703bp. Previous studies have shown that LINC02535 is highly expressed in poorly differentiated gastric cancer, which promotes cell proliferation and leads to metastasis [13]. In addition, it also plays a synergistic role with PCBP2 promoting DNA damage repair and maintaining the expression of RRM1 mRNA, thus promoting the proliferation of cervical cancer cells and the development of epithelial-mesenchymal transition (EMT) [14]. In lung cancer, LINC02535 is found to regulate NF-κB signaling pathway via miR-30a-5p/GALNT3 axis, promoting tumor growth [15]. However, to date, there are still few studies on the role of LINC02535 in diagnosis and treatment of various malignancies. Thus, the value of LINC02535 in assessing the prognosis of cancer patients and regulating tumor development has not been sufficiently understood yet.

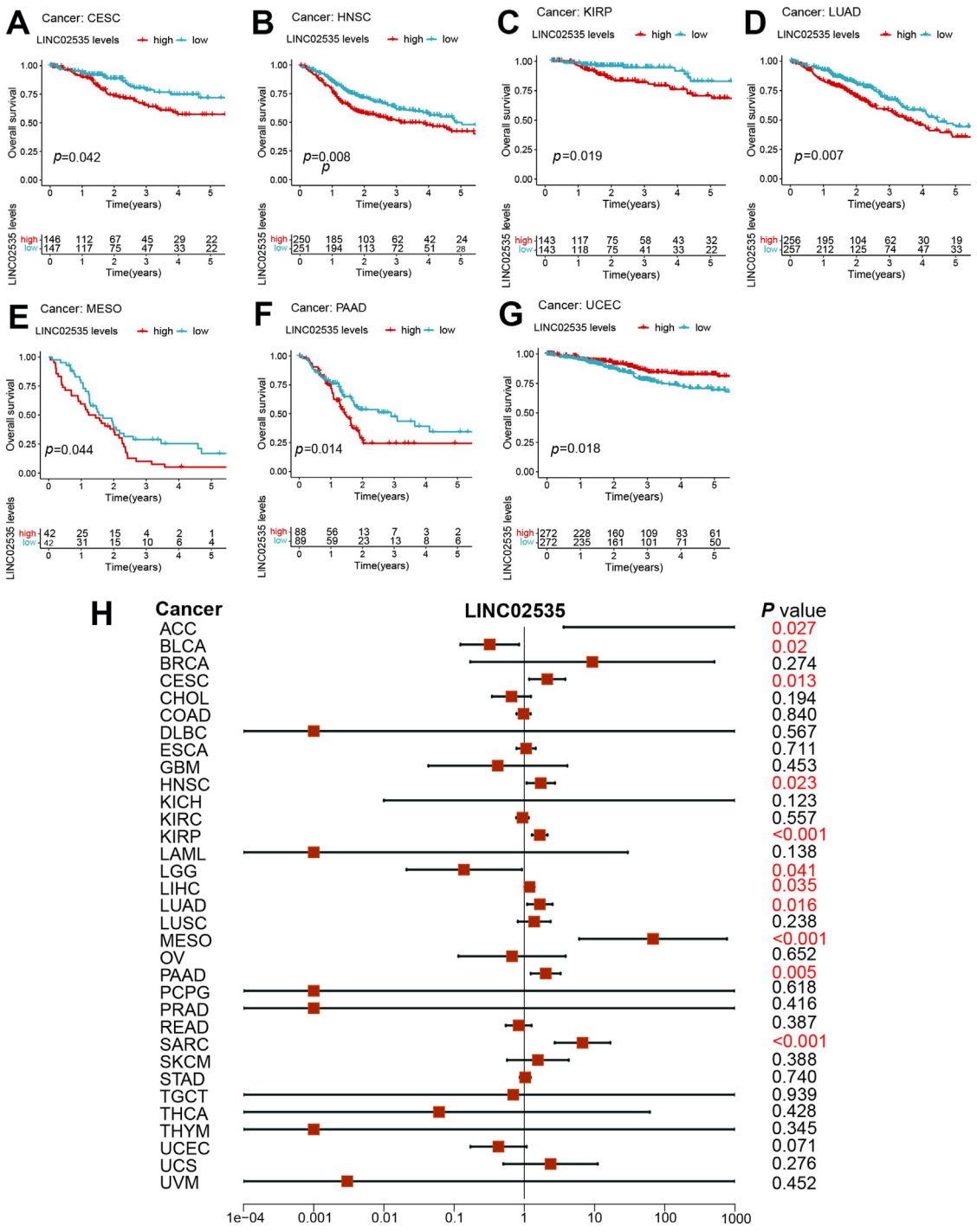

Figure 2. The association of LINC02535 with OS. (A–G) Kaplan–Meier curves of OS for CESC, HNSC, KIRP, LUAD, MESO, PAAD, and UCEC, respectively; (H) The forest plot across pan-cancer for OS analysis. OS: Overall survival; CESC: Cervical squamous cell carcinoma and endocervical adenocarcinoma; HNSC: Head and Neck squamous cell carcinoma; KIRP: Kidney renal papillary cell carcinoma; LUAD: Lung adenocarcinoma; MESO: Mesothelioma; PAAD: Pancreatic adenocarcinoma; UCEC: Uterine Corpus Endometrial Carcinoma.

Recent years have brought us into a new era in cancer research thanks to the pan-cancer analysis [16]. Herein, we performed a pan-cancer analysis of LINC02535 using the Cancer Genome Atlas (TCGA) database to explore its potential value. Most importantly, the oncogenic role of LINC02535 in lung adenocarcinoma (LUAD) has been further verified by *in vitro* and *in vivo* assays, thus providing new insights and evidence for the diagnosis and treatment of LUAD by finding new potential targets.

2. Materials and methods

2.1. Bioinformatics data acquisition

Batch effects normalized RNA-seq data of pan-cancer types and human cancer cell lines were both extracted from UCSC Xena (https://xenabrowser.net/datapages/). Cancer types were listed in Table S1. Hallmark gene list for enrichment analysis was downloaded from the

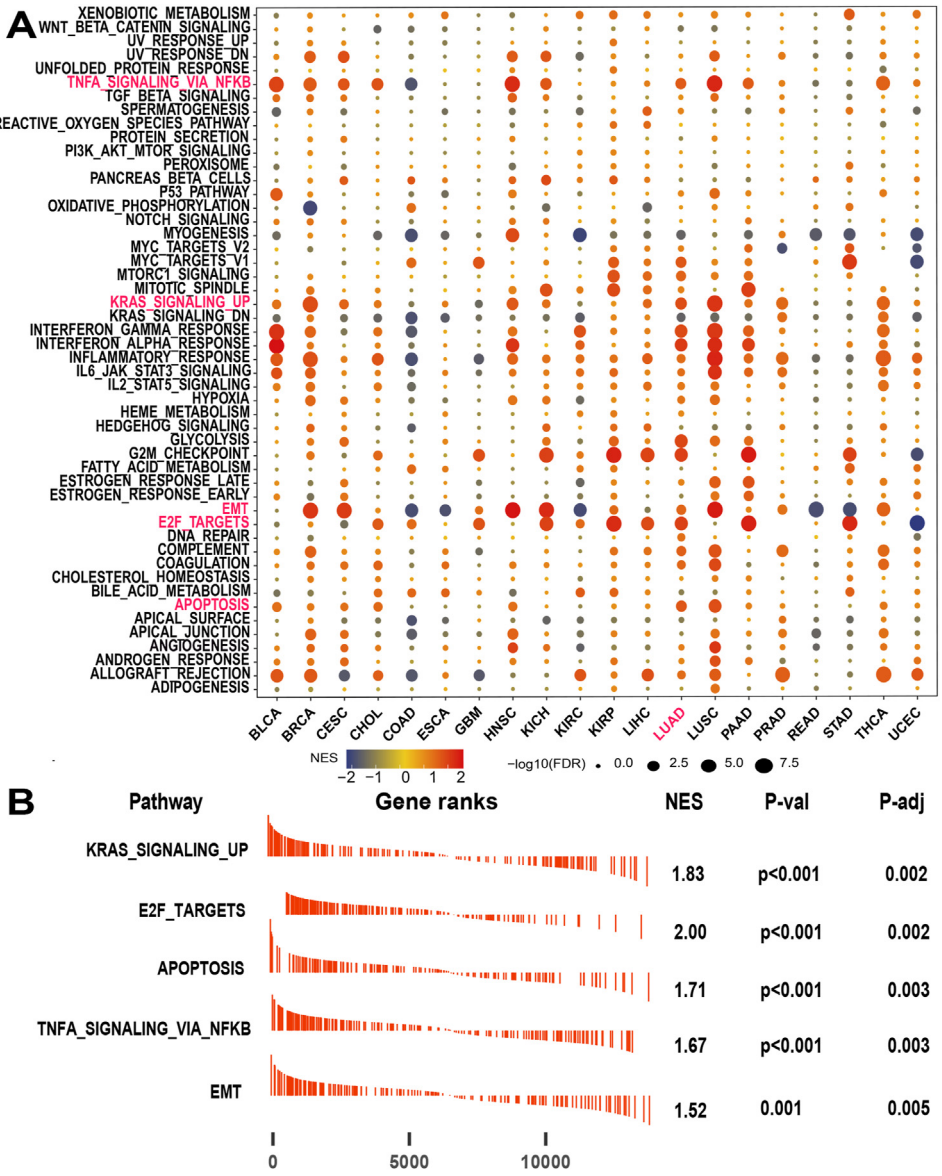

Figure 3. Function analysis of LINC02535. (A) Representative signaling pathways in pan-cancers determined by GSEA based on TCGA dataset. Pathways with "red" and "blue" color are predicted to be activated (NES>0) or inhibited (NES<0), respectively. The circle size ≥2.5 is viewed as statistical significance. (B) Representative signaling pathways in LUAD based on TCGA dataset. LUAD: Lung Adenocarcinoma.

website of GSEA (http://www.gsea-msigdb.org/gsea/index.jsp). The predictive subcellular location of LINC02535 was retrieved in lncLocator website (http://www.csbio.sjtu.edu.cn/bioinf/lncLocator/).

2.2. Differentially expressed gene analysis and survival analysis

The differentially expressed LINC02535 profiles across multiple cancer types from TCGA were analyzed by the built-in R function "wilcox.test", and visualized by using the "ggplot2" package. To investigate whether LINC02535 affects cancer progression, patients were stratified into two (stage I + II/stage III + IV) subgroups. Moreover, Kaplan–Meier analysis and Cox regression analysis of overall survival (OS) were utilized to describe the prognostic patterns of LINC02535 in multiple cancer types, with the R packages of "survival" and "survminer".

2.3. Gene set enrichment analysis and correlation analysis

Patients were divided into two subgroups according to the median value of LINC02535 expression, followed by differential analysis of all genes. Then, genes were reordered following the value of fold change calculated by the differential analysis. To investigate the role of LINC02535, gene set enrichment analysis (GSEA) algorithm of R "clusterProfiler" package was employed to analyze the normalized enrichment score (NES) of fifty hallmarks via using the "h.all.v7.4.symbols.gmt" gene set. Pathways/phenotypes were activated or suppressed in LINC02535 high expression group when NES >0 or NES <0, respectively. Based on TCGA and CCLE datasets, correlations between LINC02535 and key pathway-related genes were analyzed using Pearson's correlation analysis.

2.4. Quantitative real-time polymerase chain reaction (qRT-PCR), Western Blotting and fluorescence in situ hybridization (FISH)

Total RNA was extracted from lung cells using TRIzol reagent (Invitrogen, USA). cDNA was synthesized from whole RNA using reverse transcription kits (TaKaRa, Japan). In addition, the cDNA microarray of LUAD tissue was acquired from Shanghai Outdo Biotech Co., Ltd (LncDNA-HLugA030PG01, Shanghai, China) containing paired LUAD tissues and para-cancer tissues. qRT-PCR was performed using the TB

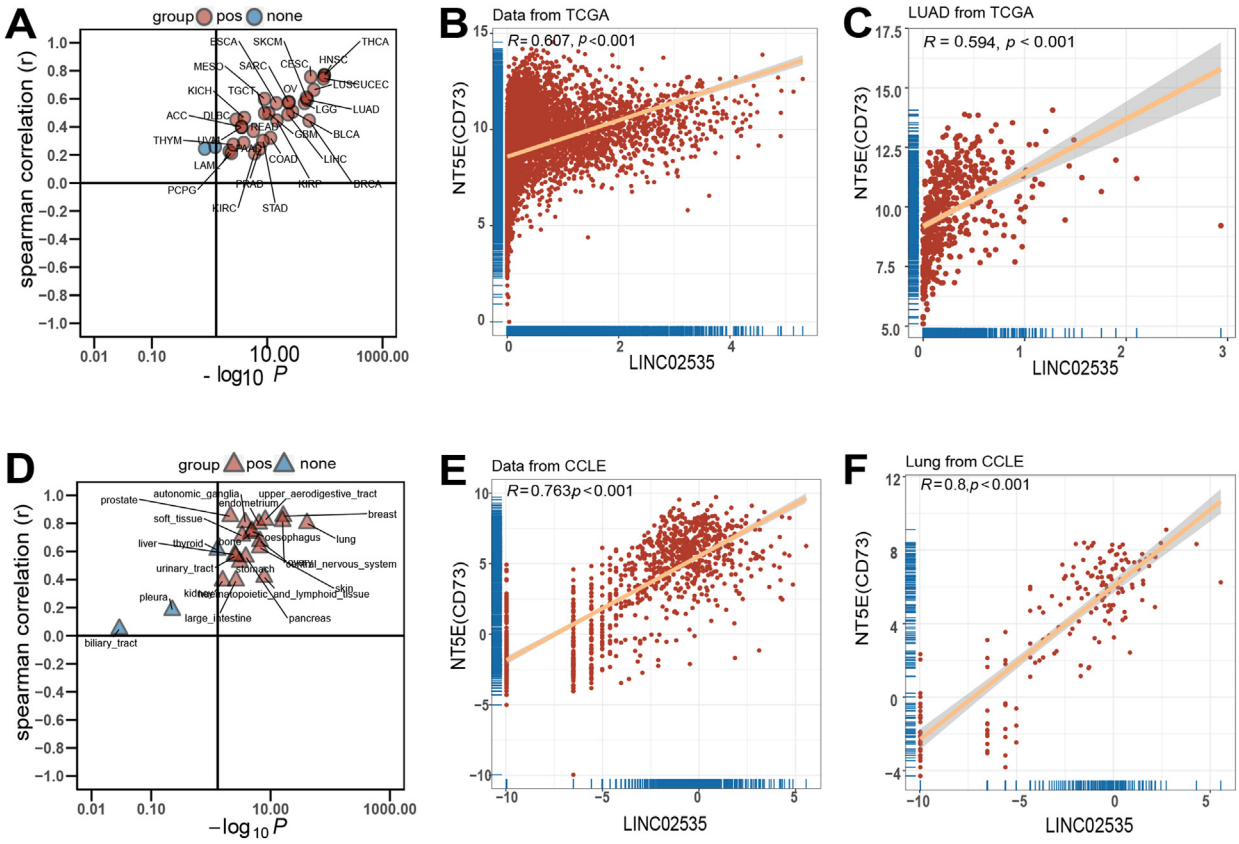

Figure 4. Coexpression analysis of LINC02535. (A–B) Significant correlations between LINC02535 and CD73 expression in pan-cancers based on TCGA dataset; (C) Strong positive correlation in LUAD based on TCGA dataset; (D–E) Significant correlations between LINC02535 and CD73 expression in human cancer cells based on CCLE dataset; (F) Strong positive correlation in LUAD cells based on CCLE dataset. LUAD: Lung Adenocarcinoma; CCLE: Cancer Cell Line Encyclopedia.

Green Premix Ex Taq (Tli RNaseH Plus) (TaKaRa, Japan) based on the product description. The primer sequences of LINC02535 and Glyceraldehyde 3-phosphate dehydrogenase (GAPDH) were acquired from Tsingke Biotechnology Co., Ltd (Table S2).

RIPA buffer (Beyotime Biotechnology, China) was used to extract total protein, followed by quantification with BCA protein assay kit (Beyotime Biotechnology, China). Subsequently, cell lysates (30 μg/per lane) were separated by SDS-PAGE on 10% gels and electronically transferred onto 0.22 μm polyvinylidene difluoride membranes. Following blocking with 5% nonfat milk at 4 °C for 60 min, the membranes were incubated with the primary antibodies rabbit monoclonal anti-Bcl-2, anti-Bax and anti-β-actin (1:1,000) overnight at 4 °C. The membranes were incubated with horseradish peroxidase-conjugated goat anti-rabbit secondary antibodies (1:5,000) for 60 min at room temperature through washing with TBS and Tween-20. The bands were tested with super-sensitive enhanced chemiluminescent kit (Zen BioScience, China). The primary antibodies rabbit monoclonal anti-Bcl-2, anti-Bax, anti-β-actin, and horseradish peroxidase-conjugated goat anti-rabbit secondary antibodies were purchased from Zen BioScience, Chengdu, China.

FISH was performed to detect the subcellular location of LINC02535. H1299 and SPCA1 cells were fixed in 4% formaldehyde, treated with pepsin, dehydrated with ethanol, and incubated with FISH probes (Guangzhou RiboBio Co., Ltd) in hybridization buffer for 24 h. After hybridization, slides were rinsed and dehydrated. DAPI (4′,6-diamidino-2-phenylindole) solution was prepared for DNA staining, followed by confocal laser scanning microscopy.

2.5. Cell culture and lentivirus transfection

Human lung cancer cell lines and bronchial epithelial cells (HBE) were purchased from the Shanghai Institutes for Biological Sciences, Chinese Academy of Sciences. These cell lines were cultured in RPMI-1640 with 10% fetal bovine serum in a humidified atmosphere of 5% CO_2 at 37 °C. H1299 and SPCA1 cells at 50%–70% of confluency were transduced with lentivirus for scramble sequence or lentivirus for expressing LINC02535 specific shRNA and then treated with puromycin (3 μg/mL) to screen stably LINC02535 silencing cells. Additionally, stably transduced cells were determined based on fluorescence intensity of green fluorescent protein (GFP) expression under a fluorescence microscope. Knockdown efficiency was calculated by qRT-PCR. The specific sequences for LINC02535 are listed in Table S3.

2.6. Cell proliferation and migration assay

The proliferative activity of stably transduced cells was tested by EdU (thymidine analogue, 5-ethynyl-2′-deoxyuridine) and clone formation assay. For EdU assay, the BeyoClick™ EdU Cell Proliferation Kit with Alexa Fluor 647 (Beyotime Biotechnology, China) is a kit based on the addition of EdU during DNA synthesis and subsequent labeling of EdU with Alexa Fluor 647 through the Click reaction to detect cell proliferation. Briefly, cells transfected with shRNA were incubated for 48 h and then treated with 20 μM EdU per well, followed by a 500 μL Click reaction cocktail for 30 min, followed by DAPI staining and observation of cells by fluorescence microscopy according to reference [17]. In terms of clone formation assay, stably transfected cells (1×10^3 cells) were cultured in triplicate in 6-well plates for 14 days. When colonies of each group were discernible, they were fixed with 4% formaldehyde for 15 min and stained with 0.5% crystal violet for 15 min. Cells were finally dried, and more than 50 cells were counted as one clone, then recorded and photographed.

All treated cells were cultured in 6-well plate and scratched with a 200 μL pipette tip in the middle of the wells, then cultured in serum-free

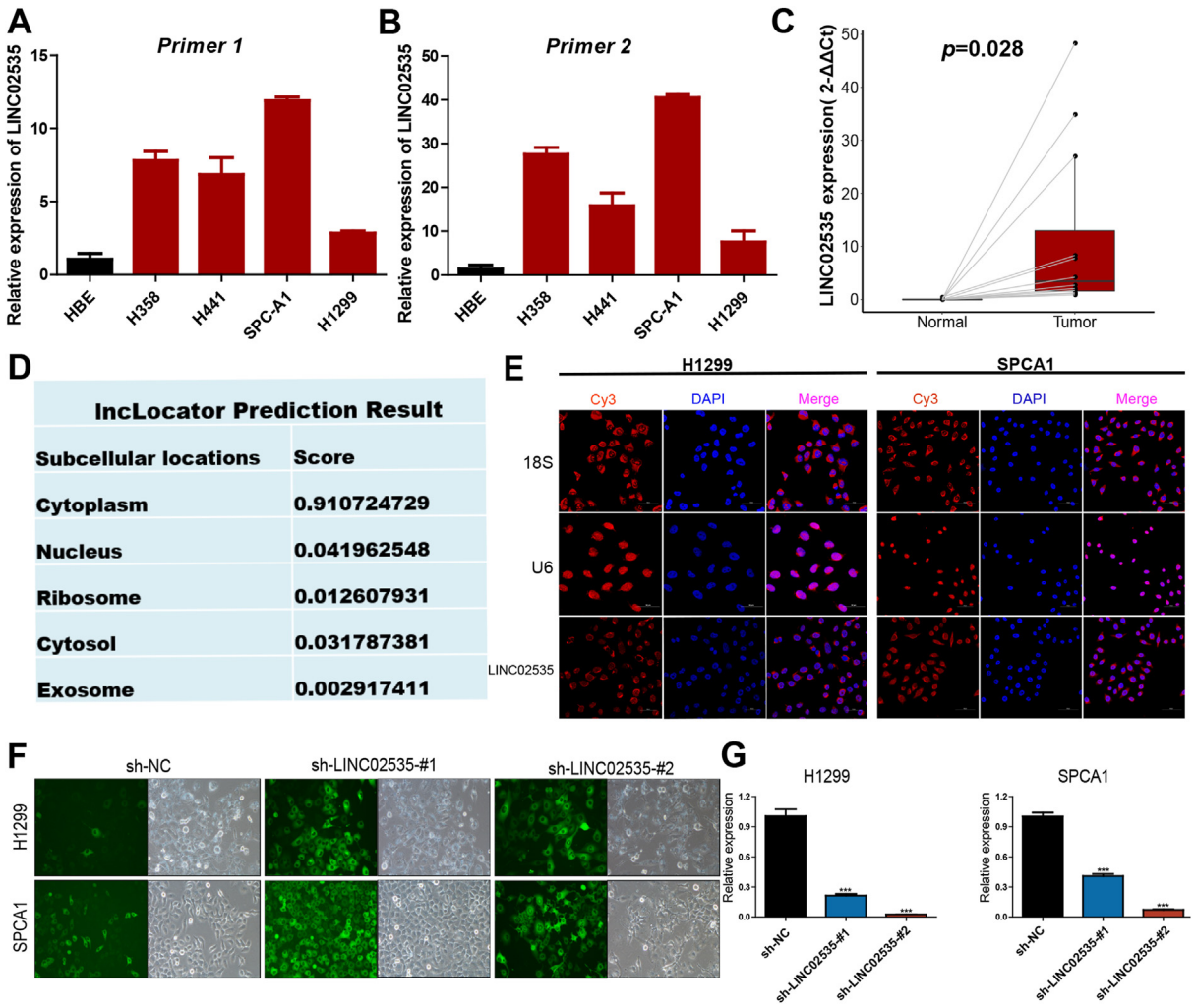

Figure 5. Expression levels and subcellular localization of LINC02535. (A–B) Expression levels of LINC02535 in different lung cancer cell lines; (C) Expression levels of LINC02535 based on LUAD cDNA microarrays; (D–E) LINC02535 is mainly localized into the cytoplasm by prediction of the lncLocator website and FISH. (F–G) Fluorescence intensity of green fluorescent protein (GFP) expression after knockdown of LINC02535. LUAD: Lung Adenocarcinoma; FISH: Fluorescence in situ Hybridization. ***$P < 0.001$.

medium. After 72 h, the width of wounds was examined in three-independent wound sites per group and normalized to control groups. For migration assay, cells suspended in 200 μL serum free medium were inoculated onto the upper chambers (BD BioCoat, MA, USA), and 500 μL medium containing 10% FBS was added to the lower chamber. After 48 h of incubation, cells were fixed with 4% paraformaldehyde for 15 min, stained with 0.5% crystal violet, and then counted under a microscope.

2.7. Xenograft model

Female BALB/C mice were purchased and fed at the State Key Laboratory of Sichuan University. The mice were randomized and injected subcutaneously with 5×10^6 SPCA1/sh-NC or SPCA1/shLINC02535 cells. The growth of tumor volume was monitored every 3 days up to 4 weeks and the tumor volume was calculated using the formula of 0.5×the longer diameter×the shorter diameter^2. The above mice were sacrificed after 28 days, and the tumor tissues were dissected and photographed for recording. This experiment was approved by the Animal Ethics Committee of Sichuan University (Approval No. 20220622004).

2.8. Cell cycle and apoptosis detected by flow cytometry

After growing for 48 h, SPCA1/sh-NC, SPCA1/shLINC02535, H1299/sh-NC, and H1299/shLINC02535 cells were collected and resuspended in 95% alcohol and fixed overnight, then incubated for 30 min with 7AAD staining solution protected from light. Cell cycle was detected by flow cytometry. Similarly, shRNA vectors were transfected into lung cancer cells. After transfection, cells were collected and resuspended in Annexin V/PE, and apoptosis was detected by flow cytometry.

2.9. Statistical analysis

All experimental data were statistically analyzed and plotted using Graphpad Prism 8. *T*-test was performed for analysis between two groups, and *F*-test for analysis between multiple groups. Each experiment was repeated at least three times. $P < 0.05$ was considered to show a statistical difference.

3. Results

3.1. LINC02535 expression in human tumors

To exhibit more accurate differentially expressed profiling, cancer types without normal tissues or with less than 5 samples were excluded. Due to the heterogeneity of gene expression across multiple samples, we performed differential analysis using the entire or paired tumor samples, respectively. LINC02535 expression was considered statistically differentially expressed only if all were validated by entire tumor samples or

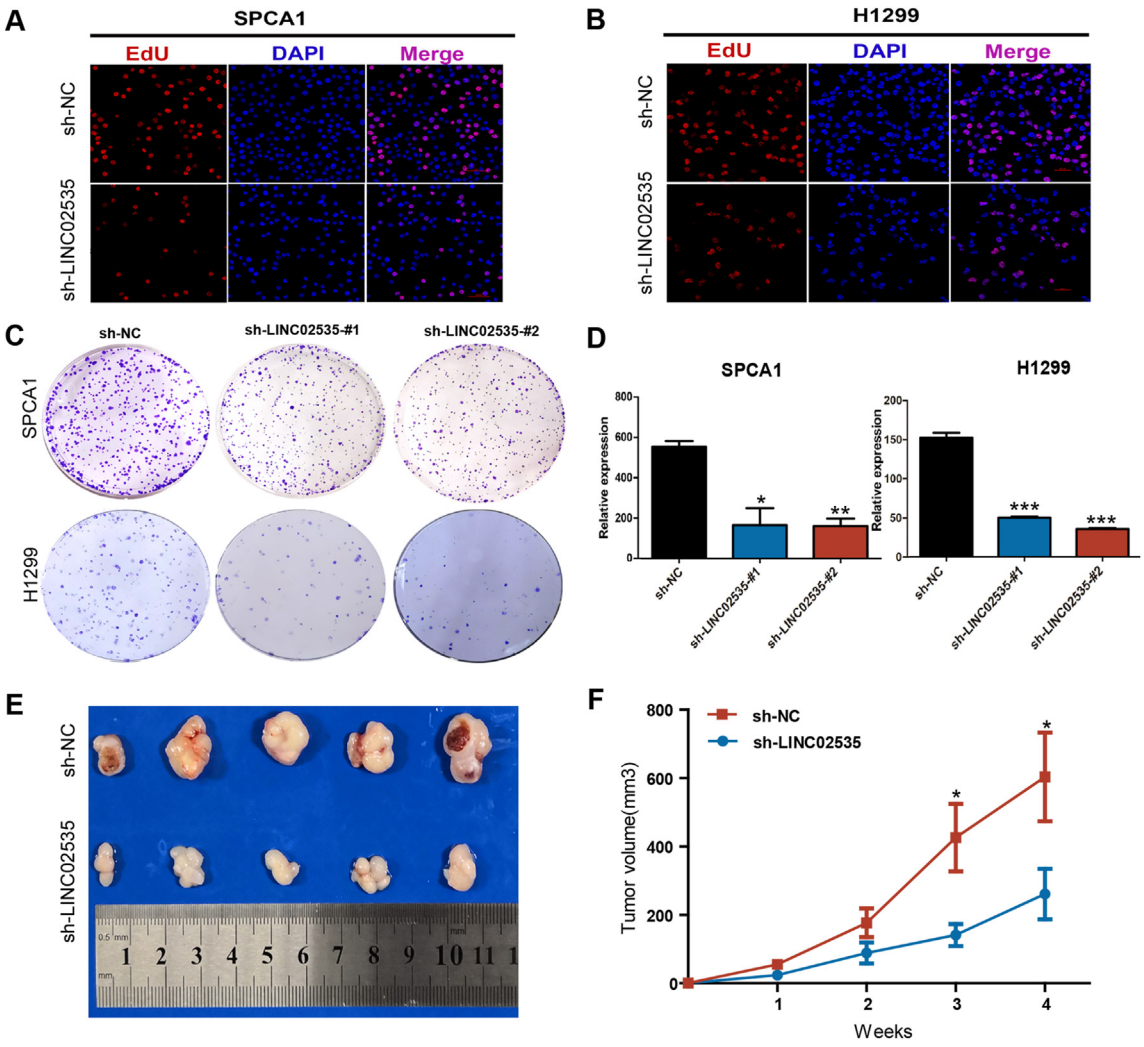

Figure 6. LINC02535 silencing suppresses cell proliferation and colony formation and retards transplanted tumor growth in LUAD. (A–B) Representative images of EdU assay; (C–D) Representative micrographs and quantification of crystal violet-stained cell clones in indicated cells; (E–F) Representative images of SPCA1 xenograted tumors from each mouse and corresponding growth curves. LUAD: Lung Adenocarcinoma. *$P < 0.05$, **$P < 0.01$, ***$P < 0.001$.

paired samples. As can be seen from Figure 1A and Figure 1B, only 10 of 17 human cancers met this condition. Specifically, LINC02535 was remarkably highly expressed in tumor tissues of head and neck squamous cell carcinoma (HNSC), LUAD, lung squamous cell carcinoma (LUSC), stomach adenocarcinoma (STAD) and thyroid carcinoma (THCA) compared with adjacent normal tissues ($P < 0.05$). However, the opposite expression level was found in tumor tissues of colon adenocarcinoma (COAD), kidney chromophobe (KICH), kidney renal clear cell carcinoma (KIRC), liver hepatocellular carcinoma (LIHC) and prostate adenocarcinoma (PRAD) ($P < 0.05$). Moreover, for kidney renal papillary cell carcinoma (KIRP) and LUAD, LINC02535 expression was significantly higher in patients with stage III + IV than those with stage I + II (Figure 1C, $P < 0.01$), but the opposite result was observed in bladder urothelial carcinoma (BLCA), breast invasive carcinoma (BRCA) and COAD ($P < 0.05$).

3.2. The predictive role of LINC02535 in human cancers

We performed survival analysis to investigate the prognostic role of LINC02535 across multiple cancers. In cervical squamous cell carcinoma and endocervical adenocarcinoma (CESC), HNSC, KIRP, LUAD, mesothelioma (MESO), and pancreatic adenocarcinoma (PAAD), Kaplan–Meier curves indicated that patients with high expression of LINC02535 survived shorter than those with low expression of LINC02535, while the opposite effect was found in uterine corpus endometrial carcinoma (UCEC) (Figure 2A–G). Similarly, Cox regression analysis suggested that LINC02535 overexpression was associated with poor prognosis in adenoid cystic carcinoma (ACC), CESC, HNSC, KIRP, LIHC, LUAD, MESO, PAAD and sarcoma (SARC). Conversely, it was found that high LINC02535 expression was linked to a greater prognosis in BLCA and brain lower grade glioma (LGG) (Figure 2H).

3.3. Identification of key signaling pathways

To investigate the potential mechanism of LINC02535, we performed GSEA based on hallmark gene sets. The heatmap indicated that proliferative or metastatic pathways/phenotypes were remarkably activated or suppressed in most cancers. LINC02535 may activate the EMT phenotype in nine cancer types including BRCA, CESC, HNSC, KICH, KIRP, LUAD, LUSC, PRAD, and THCA, as well as suppress the EMT phenotype in five cancer types including COAD, esophageal cancer (ESCA), KIRC, READ and STAD (Figure 3A). In LUAD, GSEA analysis revealed that LINC02535 may be involved in EMT, E2F targets, TNFα-NFκB and KRAS-up pathways (Figure 3B). Interestingly, the correlation analysis from TCGA cohort showed that EMT-related gene CD73 (NT5E) was highly correlated with LINC02535 in almost all cancers (Figure 4A), and the correlation coefficients were 0.607 and 0.594 in pan-cancer analysis and LUAD analysis, respectively ($P < 0.001$) (Figure 4B–C). Similarly, based on the

CCLE database, the strong correlation between CD73 and LINC02535 was observed in human cancer cells (Figure 4D). The correlation coefficients were 0.763 and 0.800 in all cancer cells and lung cancer cells, respectively ($P < 0.001$) (Figure 4E–F).

3.4. In situ expression of LINC02535

To validate the accuracy of bioinformatics analysis, we detected the *in situ* expression of LINC02535 in lung cancer cells and tissues. LINC02535 was highly expressed in lung cancer cells than in HBE cells ($P < 0.05$, Figure 5A–B). In addition, the expression of LINC02535 in 12 paired samples of lung cancer and adjacent tissues was also determined by cDNA microarrays-based qRT-PCR, consistent with the above results ($P = 0.028$, Figure 5C). To explore the potential biological function of LINC02535, the prediction of the lncLocator website and FISH were performed to test its subcellular localization, which found that it is predominantly localized into the cytoplasm (Figure 5D–E).

3.5. LINC02535 silencing inhibits the proliferation and migration of LUAD

To explore the biological function of LINC02535, cancer cells were infected with constructed lentiviral shRNA targeting LINC02535 and lentivirus containing scrambled sequence (sh-NC) (Figure 5F-G). First, cells treated with shLINC02535 and sh-NC were stained with EdU, followed by fluorescence microscopy detection. As shown in Figure 6A–B, downregulation of LINC02535 significantly inhibited the proliferative activity of SPCA1 and H1299 cells compared to sh-NC group. Similarly, LINC02535 silencing also remarkably attenuated the clonogenicity of SPCA1 and H1299 cells ($P < 0.05$, Figure 6C–D). To determine the effect of LINC02535 on tumor growth *in vivo*, SPCA1 cells treated with shLINC02535 and sh-NC were injected subcutaneously into nude mice, and the dynamic growth of implanted tumors was monitored until 4 weeks after inoculation. The dissected tumors were visualized in Figure 6E and the dynamic growth of SPCA1/shLINC02535 tumors was significantly retarded compared with that of the SPCA1/sh-NC group ($P < 0.05$, Figure 6F).

Then, scratch healing and Transwell assay were conducted to examine the impact of LINC02535 on the migration of lung cancer cells. As shown in Figure 7, compared with control groups, the migration phenotype of SPCA1/shLINC02535 and H1299/shLINC02535 were remarkably attenuated.

3.6. LINC02535 knockdown induces cell cycle arrest at G1 phase and facilitates apoptosis of lung cancer cells

To explore the mechanism underlying the phenotype of LINC02535 silencing in suppressing the proliferation of lung cancer cells, the effect of LINC02535 silencing on cell cycling and apoptosis was determined by flow cytometry. As can be seen from Figure 8A–B, percentages of SPCA1/shLINC02535 and H1299/shLINC02535 cells at phase G1 were higher than those in control groups, while percentages of SPCA1/shLINC02535 and H1299/shLINC02535 cells at phase S were lower than those in control groups ($P < 0.05$). Moreover, percentages of apoptotic SPCA1/shLINC02535 and H1299/shLINC02535 cells were higher than those in control groups ($P < 0.05$, Figure 8C–D). In parallel with the above results, Western Blotting showed that LINC02535 silencing downregulated the expression of Bcl-2, and upregulated Bax expression (Figure 8E). These findings suggested that LINC02535 may act as an upstream regulator on the G1/S transition and apoptosis of LUAD cells.

4. Discussion

LINC02535 has been regarded as a promising biomarker for gastric cancer and cervical cancer [13, 14]. Nonetheless, there were few studies of LINC02535 in other malignancies. Herein, we found that LINC02535 varied among distinct cancer types in expression level, predictive value and oncogenic pathways. Interestingly, it was observed that LINC02535 was positively correlated with CD73 (an EMT-related gene) in almost all cancer tissues or cell lines. Most importantly, we have demonstrated that LINC02535 is highly expressed in LUAD, serves as a poor prognostic factor and confers the proliferative/metastatic phenotype of LUAD by regulating apoptotic cell signaling and cell cycle signaling.

The present pan-cancer analysis indicated that the increase of LINC02535 expression in tumor was correlated with advanced TNM stage and unfavorable prognosis in LUAD and KIRP. Moreover, oncogenic pathways/phenotypes were activated in cancers with increased LINC02535 expression such as HNSC, KIRP, LUAD, LUSC and THCA, whereas most oncogenic pathways/phenotypes were suppressed in cancers with decreased LINC02535 expression such as COAD, READ and

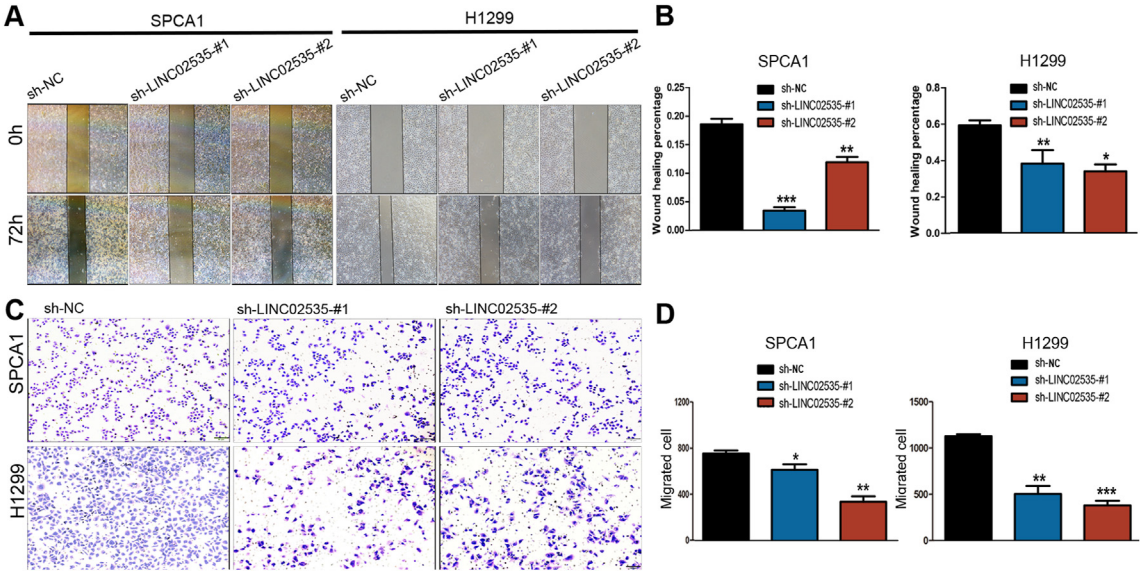

Figure 7. LINC02535 silencing inhibits cell migration in LUAD. (A–B) Representative images of scratch wound healing assay and bar plots reflecting horizontal migration of indicated cells; (C–D) Representative images of Transwell assay and bar plots reflecting vertical migration of indicated cells. LUAD: Lung Adenocarcinoma. *$P < 0.05$, **$P < 0.01$, ***$P < 0.001$.

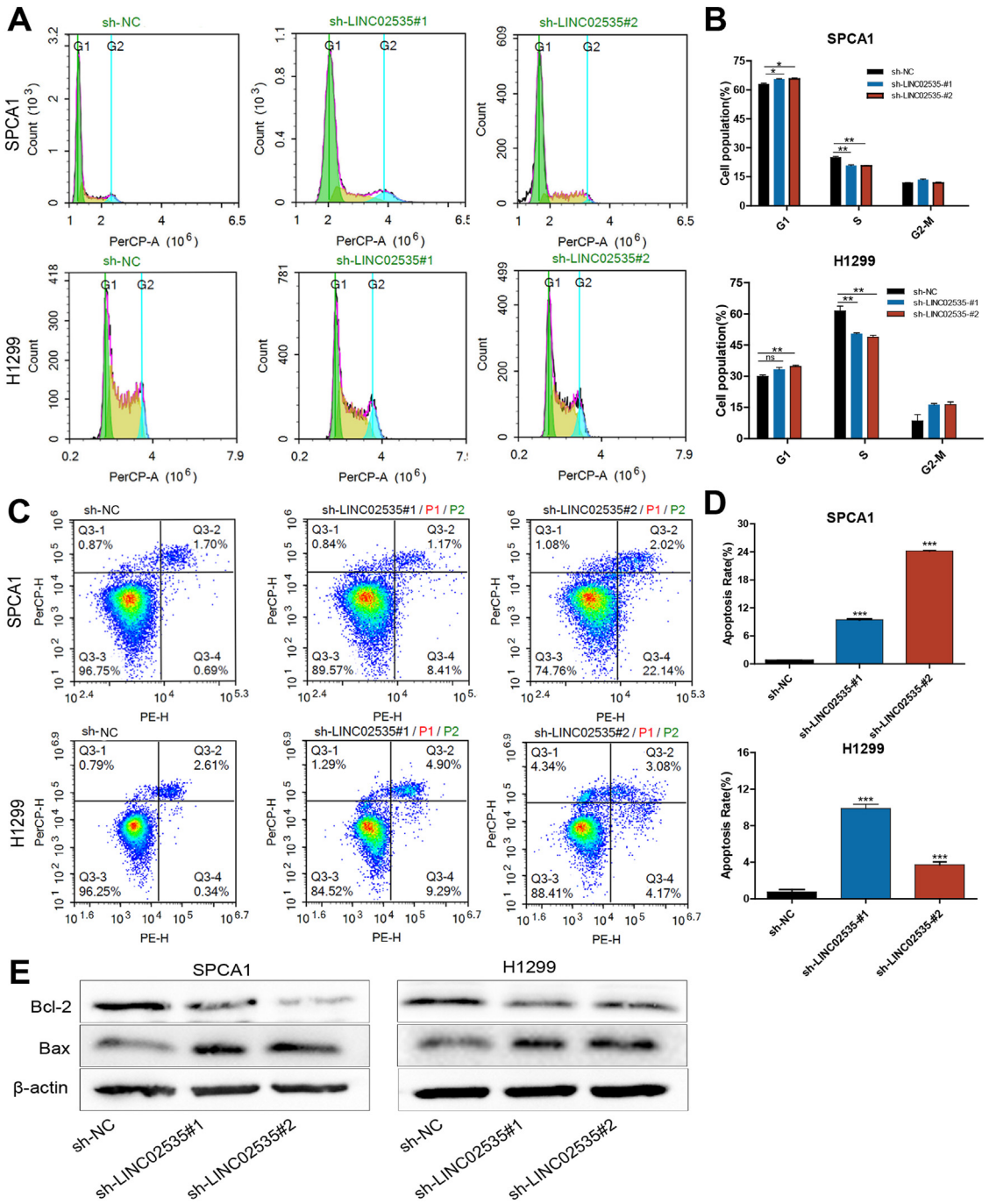

Figure 8. LINC02535 silencing delays the transition of G1 to S phase and accelerates the apoptosis of LUAD Cells. (A–B) Representative images and corresponding bar pots of flow cytometry analysis in differently treated groups; (C–D) Representative images and bar plots of proportion of apoptotic cells in differently treated groups; (E) The expression levels of apoptosis-related proteins are detected by Western Blotting. LUAD: Lung Adenocarcinoma. $^{*}P < 0.05$, $^{**}P < 0.01$, $^{***}P < 0.001$.

KIRC. These findings have not been previously reported. Recently, it's reported that LINC02535 can facilitate the progression of CESC via EMT and serve as an adverse prognostic factor [14], which is consistent with the very bioinformatic analysis results in this study. In addition, our pan-cancer analysis demonstrated that intratumoral increase of LINC02535 may promote the growth of gastric cancer for the activated oncogenic pathways including MYC target V1/V2, G2/M checkpoint and E2F targets, partly in line with the Wu et al's research [13].

EMT is a universal phenotype linked to cancer angiogenesis and metastasis, which predicts a poor prognosis [18, 19]. Herein, LINC02533 varies in the modulation of EMT across multiple cancer types, which may at least partly attribute to the varied tumor microenvironment (TME), because TCGA and CCLE databases both show that LINC02535 is positively associated with the EMT-related gene CD73 (NT5E) in almost all cancer tissues and cancer cell lines. CD73 is a major nucleoti de-metabolizing enzyme expressed in the TME and various cells such as immune cells, mesenchymal stem cells, and epithelial cells [20, 21, 22]. Compelling evidence has elucidated the impact of CD73 on EMT [23, 24, 25], suggesting that LINC02535 might facilitate the CD73 mediation of EMT. Mechanistically, CD73, as a rate limiting enzyme for adenosine production, maintains tissue homeostasis by converting CD39-ATP triggered immune response to adenosine-mediated immunosuppression

[26]. Some studies have shown that CD73 is regarded as an emerging immune checkpoint, and targeting CD73 can improve the sensitivity of immunotherapy [27, 28, 29, 30, 31]. Thus, LINC02535 provides the immunosuppressive microenvironment by modulating CD73 directly or indirectly and it has become a promising biomarker for predicting immunotherapeutic response.

In addition, LINC02535 expression was upregulated in LUAD cells, and knockdown of LINC02535 inhibited the proliferation and migration of LUAD cells in our study, suggesting that LINC02535 could be considered as a risk factor of LUAD, which was in accordance with Li et al's study [15]. Flow cytometry results found that downregulation of LINC02535 attenuated the G1/S phase transition of the cell cycling, and accelerated apoptosis. Compared to Li et al's study [15], we proposed for the first time that LINC02535 can inhibit apoptotic cell signaling and activate cell cycle signaling to promote cell growth, which further enhances the understanding that LINC2535 promotes LUAD development. Previous studies have shown that cell cycle dysregulation affects abnormal cell division, thus promoting aberrant cell growth [32]. G1/S transition is a critical step in cell proliferation and determines whether cells can enter DNA replication [33], which suggests that regulation of cell cycle is closely related to the development of LUAD, and LINC02535 may play an important role in this process. While, the exact mechanism needs to be further determined in subsequent experiments.

There are a few limitations of this study. First, further experiments in different cancers should be performed to identify the function of LINC02535 in other cancer types. Second, the expression of LINC02535 needs to be further verified by expanding LUAD tissue samples, and the underlying mechanism of LINC02535 in promoting LUAD progression is worth to be investigated. Nevertheless, the findings of our study still have noteworthy implications for the role of LINC02535 in cancers, especially in LUAD.

5. Conclusion

In summary, our study has predicted the pro-tumor and anti-tumor roles of LINC02535 across distinct cancer types, and further validated the oncogenic role of LINC02535 in LUAD via *in vitro* and *in vivo* assays. Notably, we have also highlighted that LINC02535 may promote tumor growth/metastases via triggering multiple downstream signaling pathways like apoptotic cell signaling, cell cycle and EMT signaling in LUAD. In the future, LINC02535 may be a promising predictor and new therapeutic target for cancer treatment.

Declarations

Author contribution statement

Shuang Dai; Tao Liu: Performed the experiments; Analyzed and interpreted the data; Wrote the paper.

Ying-Ying He; Yan Huang; Li Wang: Contributed reagents, materials, analysis tools or data.

Feng Luo; Yan Li: Conceived and designed the experiments.

Funding statement

Pr. Yan Li was supported by Sichuan University [2022SCUH0018].

Data availability statement

Data included in article/supp. material/referenced in article.

Declaration of interest's statement

The authors declare no competing interests.

Additional information

Supplementary content related to this article has been published online at https://doi.org/10.1016/j.heliyon.2022.e12108.

Acknowledgements

None.

References

[1] J. Ferlay, M. Colombet, I. Soerjomataram, D.M. Parkin, M. Piñeros, A. Znaor, F. Bray, Cancer statistics for the year 2020: an overview, Int. J. Cancer (2021).
[2] M.R. Cosenza, B. Rodriguez-Martin, J.O. Korbel, Structural variation in cancer: role, prevalence, and mechanisms, Ann. Rev. Genomics Hum. Genet. (2022).
[3] R.L. Siegel, K.D. Miller, A. Jemal, Cancer statistics, CA A Cancer J. Clin. 69 (2019) 7–34, 2019.
[4] C. Santucci, G. Carioli, P. Bertuccio, M. Malvezzi, U. Pastorino, P. Boffetta, E. Negri, C. Bosetti, C. La Vecchia, Progress in cancer mortality, incidence, and survival: a global overview, Eur. J. Cancer Prev. 29 (2020) 367–381.
[5] G. Di Leva, M. Garofalo, C.M. Croce, MicroRNAs in cancer, Annu. Rev. Pathol. 9 (2014) 287–314.
[6] M.K. Iyer, Y.S. Niknafs, R. Malik, U. Singhal, A. Sahu, Y. Hosono, T.R. Barrette, J.R. Prensner, J.R. Evans, S. Zhao, A. Poliakov, X. Cao, S.M. Dhanasekaran, et al., The landscape of long noncoding RNAs in the human transcriptome, Nat. Genet. 47 (2015) 199–208.
[7] Samudyata, G. Castelo-Branco, A. Bonetti, Birth, coming of age and death: the intriguing life of long noncoding RNAs, Semin. Cell Dev. Biol. 79 (2018) 143–152.
[8] W. Su, S. Feng, X. Chen, X. Yang, R. Mao, C. Guo, Z. Wang, D.G. Thomas, J. Lin, R.M. Reddy, M.B. Orringer, A.C. Chang, Z. Yang, et al., Silencing of long noncoding RNA MIR22HG triggers cell survival/death signaling via oncogenes YBX1, MET, and p21 in lung cancer, Cancer Res. 78 (2018) 3207–3219.
[9] D. Yin, X. Lu, J. Su, X. He, W. De, J. Yang, W. Li, L. Han, E. Zhang, Long noncoding RNA AFAP1-AS1 predicts a poor prognosis and regulates non-small cell lung cancer cell proliferation by epigenetically repressing p21 expression, Mol. Cancer 17 (2018) 92.
[10] Z. Peng, J. Wang, B. Shan, B. Li, W. Peng, Y. Dong, W. Shi, W. Zhao, D. He, M. Duan, Y. Cheng, C. Zhang, C. Duan, The long noncoding RNA LINC00312 induces lung adenocarcinoma migration and vasculogenic mimicry through directly binding YBX1, Mol. Cancer 17 (2018) 167.
[11] J. Yang, Q. Qiu, X. Qian, J. Yi, Y. Jiao, M. Yu, X. Li, J. Li, C. Mi, J. Zhang, B. Lu, E. Chen, P. Liu, et al., Long noncoding RNA LCAT1 functions as a ceRNA to regulate RAC1 function by sponging miR-4715-5p in lung cancer, Mol. Cancer 18 (2019) 171.
[12] G. Sturm, F. Finotello, F. Petitprez, J.D. Zhang, J. Baumbach, W.H. Fridman, M. List, T. Aneichyk, Comprehensive evaluation of transcriptome-based cell-type quantification methods for immuno-oncology, Bioinformatics 35 (2019) i436–i445.
[13] J. Wu, L. Gao, H. Chen, X. Zhou, X. Lu, Z. Mao, LINC02535 promotes cell growth in poorly differentiated gastric cancer, J. Clin. Lab. Anal. 35 (2021), e23877.
[14] D. Wen, Z. Huang, Z. Li, X. Tang, X. Wen, J. Liu, M. Li, LINC02535 co-functions with PCBP2 to regulate DNA damage repair in cervical cancer by stabilizing RRM1 mRNA, J. Cell. Physiol. 235 (2020) 7592–7603.
[15] Y. Li, J. Zhao, W. Zhang, A. Wang, M. Jiao, X. Cai, J. Zhu, Z. Liu, J.A. Huang, LINC02535/miR-30a-5p/GALNT3 axis contributes to lung adenocarcinoma progression via the NF- κ B signaling pathway, Cell Cycle (2022) 1–16.
[16] F. Dong, Pan-cancer molecular biomarkers: a paradigm shift in diagnostic pathology, Surg. Pathol. Clin. 14 (2021) 507–516.
[17] T.G. He, Z.Y. Xiao, Y.Q. Xing, H.J. Yang, H. Qiu, J.B. Chen, Tumor suppressor miR-184 enhances chemosensitivity by directly inhibiting SLC7A5 in retinoblastoma, Front. Oncol. 9 (2019) 1163.
[18] B. De Craene, G. Berx, Regulatory networks defining EMT during cancer initiation and progression, Nat. Rev. Cancer 13 (2013) 97–110.
[19] V. Mittal, Epithelial mesenchymal transition in tumor metastasis, Annu. Rev. Pathol. 13 (2018) 395–412.
[20] A. Clayton, S. Al-Taei, J. Webber, M.D. Mason, Z. Tabi, Cancer exosomes express CD39 and CD73, which suppress T cells through adenosine production, J. Immunol. 187 (2011) 676–683.
[21] T. Lu, Z. Zhang, J. Zhang, X. Pan, X. Zhu, X. Wang, Z. Li, M. Ruan, H. Li, W. Chen, M. Yan, CD73 in small extracellular vesicles derived from HNSCC defines tumour-associated immunosuppression mediated by macrophages in the microenvironment, J. Extracell. Vesicles 11 (2022), e12218.
[22] C. Brown, C. McKee, S. Bakshi, K. Walker, E. Hakman, S. Halassy, D. Svinarich, R. Dodds, C.K. Govind, G.R. Chaudhry, Mesenchymal stem cells: cell therapy and regeneration potential, J. Tissue Eng. Regen. Med. 13 (2019) 1738–1755.
[23] H.K. Oh, J.I. Sin, J. Choi, S.H. Park, T.S. Lee, Y.S. Choi, Overexpression of CD73 in epithelial ovarian carcinoma is associated with better prognosis, lower stage, better differentiation and lower regulatory T cell infiltration, J. Gynecol. Oncol. 23 (2012) 274–281.
[24] F. Xue, T. Wang, H. Shi, H. Feng, G. Feng, R. Wang, Y. Yao, H. Yuan, CD73 facilitates invadopodia formation and boosts malignancy of head and neck squamous cell carcinoma via the MAPK signaling pathway, Cancer Sci. (2022).

[25] Z.W. Gao, C. Liu, L. Yang, H.C. Chen, L.F. Yang, H.Z. Zhang, K. Dong, CD73 severed as a potential prognostic marker and promote lung cancer cells migration via enhancing EMT progression, Front. Genet. 12 (2021), 728200.
[26] M. Roh, D.A. Wainwright, J.D. Wu, Y. Wan, B. Zhang, Targeting CD73 to augment cancer immunotherapy, Curr. Opin. Pharmacol. 53 (2020) 66–76.
[27] B. Allard, S. Pommey, M.J. Smyth, J. Stagg, Targeting CD73 enhances the antitumor activity of anti-PD-1 and anti-CTLA-4 mAbs, Clin. Cancer Res. 19 (2013) 5626–5635.
[28] C.M. Hay, E. Sult, Q. Huang, K. Mulgrew, S.R. Fuhrmann, K.A. McGlinchey, S.A. Hammond, R. Rothstein, J. Rios-Doria, E. Poon, N. Holoweckyj, N.M. Durham, C.C. Leow, et al., Targeting CD73 in the tumor microenvironment with MEDI9447, OncoImmunology 5 (2016), e1208875.
[29] I. Perrot, H.A. Michaud, M. Giraudon-Paoli, S. Augier, A. Docquier, L. Gros, R. Courtois, C. Déjou, D. Jecko, O. Becquart, H. Rispaud-Blanc, L. Gauthier, B. Rossi, et al., Blocking antibodies targeting the CD39/CD73 immunosuppressive pathway unleash immune responses in combination cancer therapies, Cell Rep. 27 (2019) 2411–2425, e9.
[30] P.A. Beavis, N. Milenkovski, M.A. Henderson, L.B. John, B. Allard, S. Loi, M.H. Kershaw, J. Stagg, P.K. Darcy, Adenosine receptor 2A blockade increases the efficacy of anti-PD-1 through enhanced antitumor T-cell responses, Cancer Immunol. Res. 3 (2015) 506–517.
[31] I.C. Iser, S. Vedovatto, F.D. Oliveira, L.R. Beckenkamp, G. Lenz, M.R. Wink, The crossroads of adenosinergic pathway and epithelial-mesenchymal plasticity in cancer, Semin. Cancer Biol. (2022).
[32] L.R. Pack, L.H. Daigh, T. Meyer, Putting the brakes on the cell cycle: mechanisms of cellular growth arrest, Curr. Opin. Cell Biol. 60 (2019) 106–113.
[33] S. Hume, G.L. Dianov, K. Ramadan, A unified model for the G1/S cell cycle transition, Nucleic Acids Res. 48 (2020) 12483–12501.